

Organometallic Complexes with Biological Molecules II. Synthesis, Solid-state Characterization and *in vivo* Cytotoxicity of Diorganotin(IV)chloro and Triorganotin(IV)chloro Derivatives of Penicillin G

F. Maggio,* A. Pellerito,* L. Pellerito,*§ S. Grimaudo,† C. Mansueto‡ and R. Vitturi‡

* Università di Palermo, Dipartimento di Chimica Inorganica, 26 Via Archirafi, I-90123 Palermo, Italy, † Università di Palermo, Istituto Farmacochimico, 32 Via Archirafi, I-90123 Palermo, Italy, and ‡ Università di Palermo, Istituto di Zoologia, 18, Via Archirafi, I-90123 Palermo, Italy

Several new diorganotin(IV)chloro and triorganotin(IV)chloro penicillin G derivatives have been prepared. The isolated compounds showed 1:1 stoichiometry, with formulae $R_2SnClpenG$ and $R_3SnClpenGNa$, respectively ($penG^- = 4\text{-thia-1-azabicyclo}[3.2.0]\text{heptane-2-carboxylate}$, 3,3-dimethyl-7-oxo-6-(2-phenylacetamido) anion; $R = Me, Bu, Ph$). The coordination environment around the tin(IV) atom, in all of the complexes, was trigonal bipyramidal. Penicillin G behaved as a monoanionic, bimonodentate ligand in $R_2SnClpenG$ through the β -lactamic carbonyl and unidentate ester-type carboxylate anion, and as unidentate through the β -lactamic carbonyl in $R_3SnClpenGNa$, as inferred on the basis of IR spectra.

The rationalization of the Mössbauer parameter nuclear quadrupole splitting, ΔE ($mm\ s^{-1}$), according to the point-charge model formalism, supported such an hypothesis.

The partial atomic charges on tin atoms, Q_{Sn} , calculated for all the diorganotin(IV)chloropenG and triorganotin(IV)chloropenGNa compounds by the CHELEQ program, correlated well with the experimental ^{119}Sn Mössbauer parameter isomer shift, δ ($mm\ s^{-1}$). The δ/Q_{Sn} data for diorganotin(IV)chloropenG and for triorganotin(IV)chloropenGNa derivatives have been correlated with the δ/Q_{Sn} values of triorganotin(IV) halide, cyanide, thiocyanate and cyanate compounds, whose trigonal bipyramidal polymeric structure has been well established.

Finally, the biological activity of diorgano-

tin(IV)chloropenG and triorganotin(IV)chloropenGNa derivatives has been tested using *Ciona intestinalis* fertilized eggs at different stages of development.

Keywords: Organotin, antibiotics, penicillin G, structure, Mössbauer, point charge, infrared, toxicity, *Ciona intestinalis*

INTRODUCTION

Metallic and organometallic complexes of several antibiotics have been the aim of much research.¹⁻¹³ Bleomycin derivatives have been synthesized and characterized by several methods, owing to the increasing use of this antibiotic as an antitumor drug.¹⁴ Little attention has been devoted to the penicillin G derivatives, which, in contrast, represent a large category of semisynthetic antibiotics, depending on the nature of the groups bonded to the aminic nitrogen atom of the 6-aminopenicillic acid.

Metallic derivatives of this 6-aminopenicillic acid have been reported by Sodhi *et al.*,^{15,16} who claimed, through spectroscopic data, its behaviour as a bidentate monoanionic ligand, coordinating the metal ions through β -lactamic carbonyl $C=O$ and by deprotonation of the 6-amino group, while no involvement of the carboxylic group was observed. Metallic and organometallic D-penicillaminato derivatives have been investigated.¹⁷⁻²⁰ Barbieri *et al.*,¹⁹ by Mössbauer

§ Author to whom correspondence should be addressed.

Table 1 Analytical data for diorganotin(IV)chloro and triorganotin(IV)chloro derivatives of penicillin G^a

Compound	Analysis: Found (calcd.) (%)				
	C	H	N	Cl	Sn
Me ₂ SnClpenG	42.21 (41.77)	4.67 (4.48)	5.55 (5.41)	7.70 (6.85)	22.91 (22.93)
Bu ₂ SnClpenG	47.10 (47.90)	5.68 (5.86)	5.21 (4.66)	6.04 (5.89)	19.30 (19.72)
Ph ₂ SnClpenG	52.82 (52.41)	4.59 (4.24)	4.38 (4.37)	5.83 (5.53)	18.73 (18.50)
Me ₃ SnClpenGNa	40.73 (41.07)	4.96 (4.72)	4.97 (5.04)	6.10 (6.38)	21.72 (21.36)
Bu ₃ SnClpenGNa	50.14 (49.32)	6.84 (6.50)	4.91 (4.11)	5.53 (5.20)	17.21 (17.41)
Ph ₃ SnClpenGNa	55.32 (55.05)	4.83 (4.35)	3.63 (3.78)	4.27 (4.78)	15.78 (16.00)

^a penG⁻, penicillin G⁻

spectroscopy and in particular by applying the point-charge model formalism and lattice dynamics parameters, hypothesized the occurrence of monodimensional polymeric trigonal bipyramidal configurations, *cis*-R₂, both for Me₂Sn and Ph₂Sn-*DL*-penicillamines. Coordination

occurred through the sulphur (S) atom, the amino group and the carboxylate anion, behaving as a unidentate, ester-type, ligand. Investigations on iron(II) benzylpenicillin G have been reported by Asso *et al.*,²¹ who assumed, on the basis of IR spectroscopy, a bidentate behaviour of benzylpenicillin G through the carboxylate group and the thiazolidinic nitrogen atom.

On the other hand, preliminary results on the interaction of diorganotin(IV)chloro and triorganotin(IV)chloro moieties with a number of antibiotics and their biological activity have been the aim of several communications.²²⁻²⁴ Moreover, the biological activity of a number of organotin(IV) compounds has been tested using *Ciona intestinalis* embryos at different stages of development.^{25, 26}

Following our previous investigations, this paper deals with the synthesis and structural aspects of several diorganotin(IV)chloro and triorganotin(IV)chloro derivatives of penicillin G.

EXPERIMENTAL

R₂SnClpenG and R₃SnClpenGNa compounds were obtained by refluxing methanolic solutions of R₂SnCl₂ or R₃SnCl (gifts from Schering AG, Bergkamen, Germany) with methanolic suspensions of penicillinGNa, (ICN, USA), in the molar ratio 1:1 {penG⁻ = penicillin G⁻ = 4-thia-1-azabicyclo[3.2.0]heptane-2-carboxylate,

3,3-dimethyl-7-oxo-6-(2-phenylacetamido) anion; R = Me, Bu, Ph}. On cooling, the compounds precipitated and the solids, recovered by filtration, were recrystallized from methanol and analyzed for C, H, N, Sn and Cl contents (Table 1). C, H and N analyses were performed at Laboratorio di Chimica Organica (University of Milano). Sn and Cl contents were determined in our laboratory according to standard methods.^{27, 28}

Infrared spectra were recorded, as Nujol and hexachlorobuadiene mulls, on a Perkin-Elmer grating spectrometer (model 983 G), between CsI windows. The spectra were analysed through a Perkin-Elmer 3600 data station with Perkin-Elmer PE 983 software (Table 2).

The ¹¹⁹Sn Mössbauer spectra (Table 3) were measured with a Laben 8001 multichannel analyser and MWE (Munchen) MR 250 driving unit, FG2 digital function generator and MA 250 velocity transducer, moving at linear velocity, constant acceleration, in a triangular waveform. A DN700 Oxford cryostat with a DTC 2 temperature controller was used to maintain the absorber samples (absorber thickness 0.5–0.6 mg ¹¹⁹Sn cm⁻²) at the temperature of liquid nitrogen.

The biological activity of penGNa, R₂SnClpenG and R₃SnClpenGNa (R = Me, Bu, Ph) was tested towards *Ciona intestinalis* specimens, collected from the Gulf of Palermo. Eggs and sperm gametes were removed from the gonoducts using steel needles. Fertilization was carried out in Millipore-filtered seawater (MFSW). Each experiment was repeated four times.

Fifteen minutes after fertilization, some of the eggs were transferred in the compound solutions (10⁻⁵ and 10⁻⁷ mol dm⁻³) and allowed to develop

until the remainder (used as controls) were swimming larvae. Embryos at gastrula and neurula stage, incubated in the same solutions for one hour, were then always transferred into normal seawater. All the experiments were performed at 27°C.

Solutions of 10^{-5} and 10^{-7} mol dm $^{-3}$ penGNa, R₂SnClpenG and R₃SnClpenGNa were prepared in Millipore-filtered seawater (pH 7.76–7.78) by diluting fresh concentrated stocks, obtained by dissolving stoichiometric amounts of each compound. Tin contents were assayed using a model 372 Perkin–Elmer atomic absorption spectrophotometer equipped with a graphite furnace.

In vivo observations were made with a Leitz microscope and photographs were taken with a Leitz orthoplan microscope, using an Ilford FP4 Plus film.

RESULTS AND DISCUSSION

Chemical investigations

1. Infrared data

The more relevant bands present in the IR spectra of penGNa, and of the new organotin(IV)-chloro derivatives synthesized, are reported in Table 2.

The binding mode of penG $^{-}$ can be interpreted by observing some of its characteristic absorption bands.

Particularly, diagnostics are the strong bands attributable, in penG $^{-}$, to ν_{NH} at 3347(s) cm $^{-1}$, β -lactamic $\nu_{\text{C=O}}$ at 1778(s) cm $^{-1}$, amidic $\nu_{\text{C=O}}$ at 1697(s) cm $^{-1}$, $\nu_{\text{asCOO}^{-}}$ at 1621(s) cm $^{-1}$, ($\delta_{\text{NH}} + \nu_{\text{CN}}$) at 1501(s) cm $^{-1}$ and $\nu_{\text{symCOO}^{-}}$ at 1419(s) cm $^{-1}$. The shift of the absorptions of the peptidic ν_{NH} , at 3297(s, bd), 3301(s, bd) and 3311(s, bd) cm $^{-1}$, in Me₂SnClpenG, Bu₂SnClpenG and Ph₂SnClpenG, respectively, together with those due to amidic $\nu_{\text{C=O}}$ [1642(s, bd) cm $^{-1}$ in Me₂SnClpenG, 1641(s, bd) cm $^{-1}$ in Bu₂SnClpenG and 1641(s, bd) cm $^{-1}$ in Ph₂SnClpenG, bands which contain also a contribution from $\nu_{\text{asCOO}^{-}}$; Table 2] are probably a consequence of intermolecular hydrogen bonding in all of the derivatives. Such interactions have been shown, *inter alia*, in penGK by Dexter *et al.* by X-ray conformational investigations.²⁹

The shifts of the β -lactamic $\nu_{\text{C=O}}$, of the asymmetric and symmetric carboxylate stretchings [1642(s, bd), 1494(m) and 1367(s) cm $^{-1}$ in

Me₂SnClpenG; 1641(s, bd), 1495(m) and 1367(s) cm $^{-1}$ in Bu₂SnClpenG; 1641(s, bd), 1494(m) and 1368(s) cm $^{-1}$ in Ph₂SnClpenG] would imply coordination of tin atoms, by penG $^{-}$, through both the β -lactamic C=O^{15, 16} and the carboxylate group. On the other hand, $\Delta\nu = (\nu_{\text{asCOO}^{-}} - \nu_{\text{symCOO}^{-}})$ values are diagnostic of the COO $^{-}$ binding mode.^{30, 31} In all the R₂SnClpenG derivatives, $\Delta\nu$ values (Table 2) are characteristic of a unidentate ester-type carboxylate group.^{32, 33}

In R₃SnClpenGNa complexes, ν_{NH} occurred (present at 3297(s, bd) cm $^{-1}$ in Me₃SnClpenGNa, at 3310(s, bd) cm $^{-1}$ in Bu₃SnClpenGNa and at 3347(s) cm $^{-1}$ in Ph₃SnClpenGNa), and in the β -lactamic and amidic $\nu_{\text{C=O}}$ (1750(s) and 1660(s); 1740(s) and 1660(s); 1740(s) and 1670(s) cm $^{-1}$), as shown in Table 2. No variation occurs in any of the R₃SnClpenGNa complexes, in respect to penG $^{-}$, for the asymmetric and symmetric carboxylate absorptions; $\Delta\nu$ values (Table 2) for these complexes exclude carboxylate anion involvement in coordination. PenG $^{-}$ behaves towards the tin atom, as a neutral unidentate ligand, through the β -lactamic C=O.

As far as the β -lactamic $\nu_{\text{C=O}}$ shifts are concerned, both for diorganotin(IV)chloropenG and triorganotin(IV)chloropenGNa derivatives, it is noteworthy that coordination of β -lactamic C=O is, normally, revealed by a $\nu_{\text{C=O}}$ decrease greater than 100 cm $^{-1}$.^{15, 16} Lower shift values are interpreted as the result of electron withdrawal from the β -lactamic C=O, owing to the involvement of the thiazolidinic nitrogen atom in coordination.²¹

In all of the R₂SnClpenG and R₃SnClpenGNa derivatives investigated, the thiazolidinic nitrogen atom of the ligand is not involved in coordination, which can be shown by the lack of significant shifts of [$\delta_{\text{NH}} + \nu_{\text{CN}}$ (amide II)] bands²¹ and CN stretchings,^{15, 16} which occurred at 1501 and 1026 cm $^{-1}$, respectively, in penGNa (Table 2). Coordination of the thiazolidinic sulphur atom could also be excluded on the basis of the occurrence of absorption bands, due to ν_{CS} ,¹⁵ at 580–582(s) cm $^{-1}$, both in the free and coordinated penGNa.

In the 600–450 cm $^{-1}$ region there are bands present which can be assigned to ν_{asSnC_2} , ν_{symSnC_2} and ν_{SnCl} ^{32–37} in the dialkyl- and trialkyltin(IV)chloro derivatives, and to tin–phenyl γ -mode in Whiffen's notation,³⁸ in diphenyltin(IV)chloropenG and triphenyltin(IV)chloropenGNa, respectively.

As far as trimethyltin(IV)chloropenGNa and

Table 2 Tentative assignment of the more relevant absorption bands (cm^{-1}) of the free and coordinated penGNa in the 4000–250 cm^{-1} region^a

Compound							
	penGNa	Me ₃ SnCpenG	Bu ₃ SnCpenG	Ph ₃ SnCpenG	Me ₃ SnCpenGNa	Bu ₃ SnCpenGNa	Ph ₃ SnCpenGNa
ν_{NH} (amide)	3354s	3297s, bd	3301s, bd	3311s, bd	3297s, bd	3310s, bd	3347s, bd
$\nu_{\text{C=O}}$ (β -lactam)	1778s	1741s	1741s	1741s	1750s	1740s	1745s
$\nu_{\text{C=O}}$ (amide I)	1697s				1660s	1660s	1670s
$\nu_{\text{C=O}}$ (amide I) + ν_{COO^-}	1642s, bd	1641s, bd	1641s, bd				
ν_{asCOO^-}	1621s				1620s	1618s	1620s
$\delta_{\text{NH}} + \nu_{\text{CN}}$ (amide II)	1501s	1494m	1495m	1494m	1501m	1500m	1500m
ν_{symCOO^-}	1419s	1367s	1367s	1368s	1437s	1432s	1430s
ν_{CN}	1026m	1030m	1030m	1028m	1026m	1030m	1027m
ν_{CS}	582s	580s	582s	581s	580s	581s	582s
ν_{asSnC_2}		559m	554m		550s	525s	
ν_{symSnC_2}		525m	530w				
$\nu_{\text{Y-Ph}}$				454s			450s
ν_{SnCl}		273w	277w	277w	290w	270s	270s
$\Delta\nu$ (cm ⁻¹)	202	275	274	273	197	186	190

^a Nujol and hexachlorobutadiene mulls: s, strong, m, medium; w, weak; bd, broad.

Table 3 Experimental Mössbauer parameters, isomer shift δ (mm s^{-1}) and nuclear quadrupole splittings ΔE_{exp} (mm s^{-1}) Γ_1 and Γ_2 measured at liquid nitrogen temperature and nuclear quadrupole splittings according to the point-charge formalism applied to the idealized structures of Fig. 1(a–f)

Compound ^a	δ	$ \Delta E_{\text{exp}} $	Γ_1	Γ_2	Structure in Fig. 1	ΔE_{calcd}
$\text{Me}_2\text{SnClpenG}$	1.26	3.29	0.98	0.96	a	3.17
					b	3.25
					c	3.13
$\text{Bu}_2\text{SnClpenG}$	1.30	3.22	0.81	0.83	a	3.17
					b	3.25
					c	3.13
$\text{Ph}_2\text{SnClpenG}$	1.21	2.79	0.90	0.92	a	2.71
					b	2.86
					c	2.76
$\text{Me}_3\text{SnClpenGNa}$	1.36	3.48	0.86	0.87	d	−3.71
					e	−4.09
					f	2.36
$\text{Bu}_3\text{SnClpenGNa}$	1.44	3.30	0.86	0.85	d	−3.71
					e	−4.09
					f	2.36
$\text{Ph}_3\text{SnClpenGNa}$	1.30	2.93	0.91	0.93	d	−3.26
					e	−3.90
					f	2.07

^a Sample thickness ranged between 0.50 and 0.60 $\text{mg } ^{119}\text{Sn cm}^{-2}$; isomer shift, $\delta \pm 0.03 \text{ mm s}^{-1}$ with respect to RT BaSnO_3 ; Γ_1 and Γ_2 values are the full width at half height of the resonant peaks, respectively at greater and lower velocity with respect to the centroid of the Mössbauer spectra; nuclear quadrupole splittings, $\Delta E \pm 0.02 \text{ mm s}^{-1}$; the partial quadrupole splitting values (pqs) in mm s^{-1} , used for calculation of theoretical ΔE are discussed in the text.

tributyltin(IV)chloropenGNa complexes are concerned, the occurrence of only one, asymmetric, ν_{SnC_2} (Table 2) is indicative of a trigonal equatorial, planar, R_3Sn configuration with local D_{3h} symmetry.

These IR findings, therefore, would suggest that the tin(IV) atom achieves, both in $\text{R}_2\text{SnClpenG}$ and in $\text{R}_3\text{SnClpenGNa}$ complexes, a coordination number of five.

2. Mössbauer data

The occurrence, in all of the investigated compounds, of only one absorbing tin(IV) species has been evidenced by the full-width values, Γ (mm s^{-1}) calculated at half-height of the resonant peaks (Table 3).³⁹

The isomer shift, δ (mm s^{-1}) (Table 3) of $\text{R}_2\text{SnClpenG}$ and $\text{R}_3\text{SnClpenGNa}$ follows the meaning of the parameter, increasing with the charge density on the tin(IV) atom on going from the phenyl- to the butyl-tin(IV) derivatives.^{40, 41}

Nuclear quadrupole splitting data (Table 3), ΔE (mm s^{-1}), lie within the values reported,

both for $\text{R}_2\text{Sn(IV)}$ and $\text{R}_3\text{Sn(IV)}$ derivatives, characterized by trigonal bipyramidal configurations.^{40, 41}

Calculated C–Sn–C angles for $\text{Me}_2\text{SnClpenG}$, $\text{Bu}_2\text{SnClpenG}$ and $\text{Ph}_2\text{SnClpenG}$ (127.7° , 125.9° and 125.8° , respectively) were in good agreement with the expected C–Sn–C angles for the *cis*- R_2 trigonal bipyramidal configuration.⁴⁰

According to the above evidence, rationalization of the nuclear quadrupole splittings, ΔE , according to the point-charge model formalism^{40–43} (PCF) has been applied to the idealized structures of Fig. 1(a–f).

The results, shown in Table 3, allow experimental and calculated ΔE to be compared. The difference between experimental and calculated ΔE values must be within the range $\pm 0.4 \text{ mm s}^{-1}$, if the hypothesized configurations are to be accepted.^{40–43}

On this basis, as far as $\text{R}_2\text{SnClpenG}$ derivatives are concerned, no choice is possible among the structures of Fig. 1(a–c), Table 3, which are all *cis*- R_2 but with different arrangements of Cl,

O(=C) and O(CO)⁻ atoms. The structure of Fig. 1(a), on the basis of literature reports, is the most probable.^{44, 45}

A better test could be proposed for the structures of R₃SnClpenGNa derivatives.

While *fac*-R₃SnO(=C)Cl and T-shaped R₃SnO(=C)Cl trigonal bipyramidal configurations (Fig. 1(e,f) could be ruled out (see ΔE_{calcd} reported in Table 3), the equatorial R₃SnO(=C)Cl structure (Fig. 1d) is more likely to be assumed.

The partial quadrupole splittings (pqs), mm s⁻¹, $\{[\text{Alk}]^{\text{tbc}} = -1.13; \{\text{Ph}\}^{\text{tbc}} = -0.98; \{\text{Alk}\}^{\text{tba}} = -0.95; \{\text{Ph}\}^{\text{tba}} = -0.89; \{\text{COO}\}_{\text{Junid}}^{\text{tba}} = -0.10; \{\text{Cl}\}^{\text{tbc}} = 0.20; \{\text{Cl}\}^{\text{tba}} = 0.20; \{\text{C=O}\}_{\text{lactamic}}^{\text{tba}} = \{\text{C=O}\}_{\text{DMA}}^{\text{tba}} = 0.10; \{\text{C=O}\}_{\text{lactamic}}^{\text{tbc}} = \{\text{C=O}\}_{\text{DMA}}^{\text{tbc}} = 0.407]$, which have been used in the application of the PCF were literature or calculated values.^{19, 40-43, 46, 47}

Such structural hypotheses, for all of the compounds synthesized, have been confirmed by the linear correlation found between the isomer shifts, δ , and the partial atomic charge on tin atoms, Q_{Sn} (Table 4; Fig. 2), computed according to tbp valence bond structures, by using appropriate bond orders and formal charges on diorganotin(IV)chloropenG (Fig. 3a), and triorganotin(IV)chloropenGNa (Fig. 3b), by an orbital electronegativity equalization procedure.⁴⁸⁻⁵¹

Furthermore, in Table 5 are reported values of Q_{Sn} (CHELEQ) on the atoms bonded to the central tin atom in the diorganotin(IV)chloropenG and triorganotin(IV)chloropenGNa, obtained with the above-mentioned procedure. For comparison purposes in Fig. 2 points 1-7 are also reported, which refer to a homologous series of triorganotin(IV) derivatives whose trigonal bipyramidal polymeric structures, with equatorial R₃Sn, have been determined by X-ray investigations or other spectroscopic techniques.^{43, 52-64}

The isomer shifts, δ , and Q_{Sn} values are averages of the Me₃Sn, Bu₃Sn and (whenever possible) also of Et₃Sn, Oct₃Sn, Pr₃Sn and, finally, Cy₃Sn derivatives.

Figure 2 shows the straight line obtained in the triorganotin(IV) series (points 1-7, □; correlation coefficient $r = 0.857$). The data δ/Q_{Sn} which refer to Alk₃SnClpenGNa and Ph₃SnClpenGNa (points 8 and 9) and to Alk₂SnClpenG and Ph₂ClpenG (points 10 and 11) fitted quite well with the line of triorganotin(IV) derivatives in Fig. 2, suggesting analogous solid-state structures.

As far as diorganotin(IV) chloropenG derivatives are concerned, polymerization could occur through bis-monodentate behaviour of the ligand penG⁻, as demonstrated by IR spectroscopy (Fig. 4a).

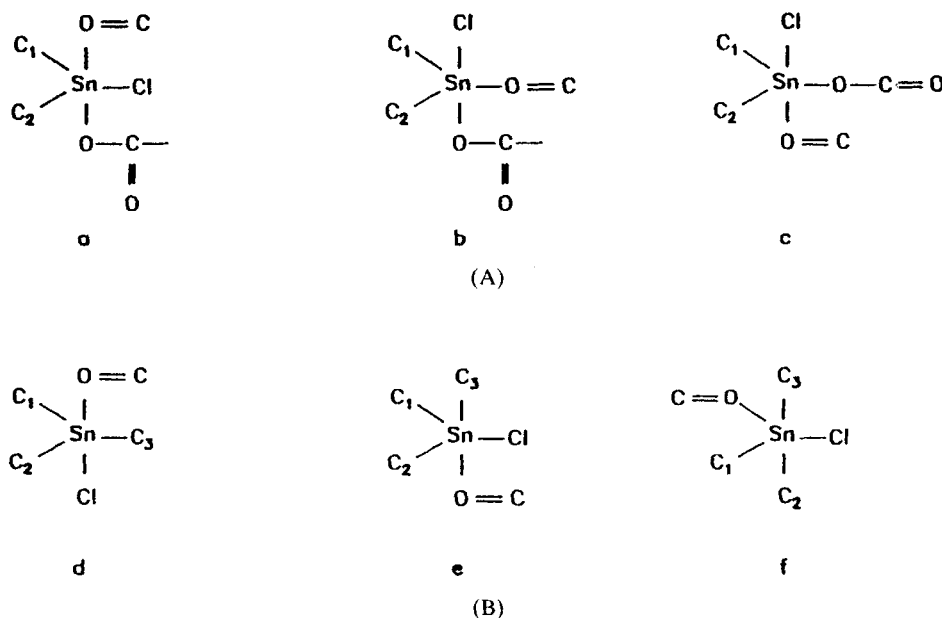


Figure 1 Idealized structures of (A) the R₃SnClO₂ group in R₃SnClpenG (a-c); (B) the R₃SnClO group in R₃SnClpenGNa (d-f). The R groups are represented by C₁, C₂ and C₃.

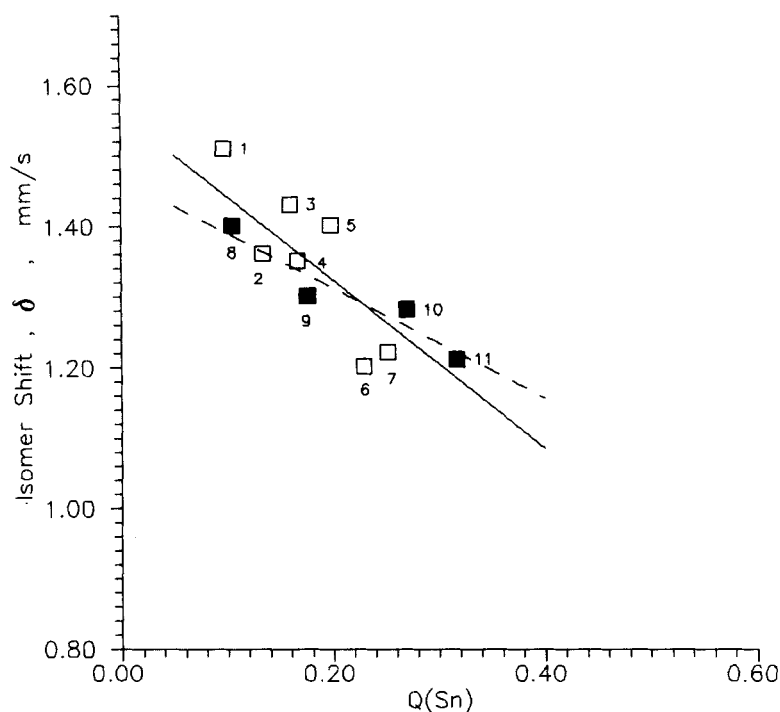


Figure 2 Correlation between the isomer shift, δ (mm s^{-1}) and Q (partial atomic charge on tin atoms (CHELEQ), for several triorganotin(IV) complexes (points 1–7, Table 4; \square) with well-ascertained polymeric trigonal bipyramidal configurations. Points 8–11 (Table 4; \blacksquare) refer to the complexes reported in this work. Full and broken lines refer to the least-squares fit treatment of points 1–7 and 8–11 from Table 4. The related equations and correlation coefficients (r) are, respectively,

$$\begin{aligned}\delta_{1-7} &= 1.584 - 1.281Q_{\text{Sn}}, r = 0.857 \\ \delta_{8-11} &= 1.514 - 0.939Q_{\text{Sn}}, r = 0.978\end{aligned}$$

Polymerization in triorganotin(IV)chloropenGNa could be achieved through hydrogen bonding between amidic NH of one

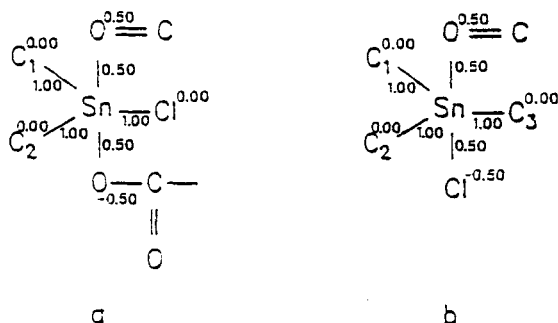


Figure 3 Trigonal bipyramidal configuration assumed for diorganotin(IV)chloropenG (a) and triorgano tin(IV)chloropenGNa complexes, points 8–11 (Table 4) together with bond orders and formal charges used for calculation of Q_{Sn} (CHELEQ).^{48–51}

Table 4 Experimental Mössbauer parameter, isomer shift δ (mm s^{-1}) and calculated partial charge on tin atoms, Q_{Sn} (CHELEQ),^{46–49} for homologous series of penta-coordinated triorganotin(IV) and diorganotin(IV) derivatives

Compound ^a	δ	Q_{Sn}	Point no. ^c	Refs for δ^b and Q_{Sn}^b
Alk_3SnCl	1.51	0.097	1	58
Alk_3SnCN	1.36	0.134	2	58
Alk_3SnNCO	1.43	0.160	3	58
Ph_3SnCl	1.35	0.167	4	64
Ph_3SnNCS	1.40	0.198	5	58
Ph_3SnNCO	1.20	0.229	6	58
Ph_3SnF	1.22	0.252	7	58
$\text{Alk}_3\text{SnClpenGNa}$	1.40	0.128	8	This work
$\text{Ph}_3\text{SnClpenGNa}$	1.30	0.208	9	This work
$\text{Alk}_3\text{SnClpenG}$	1.28	0.270	10	This work
$\text{Ph}_2\text{SnClpenG}$	1.21	0.317	11	This work

^a See discussion in the text. ^b Average of the δ and Q_{Sn} (CHELEQ) values reported in the cited references.

^c Identification numbers of the points reported in Fig. 2.

Table 5 Calculated Q (CHELQ)^{48, 51} values for the atoms bonded to the tin(IV) atoms, according to structures, bond orders and charges of Fig. 3(a, b)

Compound ^a	Q						
	Sn	C ₁	C ₂	C ₃	Cl	⁻ O—C=O	O=C (β lactamic)
Me ₂ SnClpenG	0.268	-0.024	-0.025		-0.093	-0.516	-0.040
Bu ₂ SnClpenG	0.271	-0.011	-0.011		-0.093	-0.516	-0.040
Ph ₂ SnClpenG	0.317	-0.042	-0.042		-0.091	-0.515	-0.051
Me ₂ SnClpenGNa	0.150	-0.028	-0.028	0.018	-0.507		-0.042
Bu ₂ SnClpenGNa	0.105	-0.017	-0.017	-0.464	-0.509		-0.042
Ph ₂ SnClpenGNa	0.208	-0.009	-0.009	-0.110	-0.506		-0.042

^a penG⁺, penicillin G⁻.

R₃SnClpenGNa unit with the peptidic C=O of another, etc. (Fig. 4b).

Finally, it is remarkable that the data points 8–11, which refer to Alk₃SnClpenGNa, Ph₃SnClpenGNa, Alk₂SnClpenG and Ph₂SnClpenG, respectively, lie on a line (the broken line, with $r=0.978$ in Fig. 2), confirming the occurrence, for all of the compounds, of similar structures.^{51, 59, 60}

Biological investigations

The biological effects of penGNa, R₂SnClpenG and R₃SnClpenGNa described in this investigation are briefly summarized as follows:

PenGNa

Eggs incubated in 10⁻⁵ and 10⁻⁷ mol dm⁻³ penGNa solutions for 15 min after fertilization (uncleaved eggs) or at the two-cell stage developed regularly. In fact, as observed in the controls (Fig. 5), the larvae obtained from the treated embryos were normal and swimming (Fig. 6).

Me₂SnClpenG

Eggs incubated for 15 min after fertilization in 10⁻⁵ and 10⁻⁷ mol dm⁻³ Me₂SnClpenG solutions cleaved regularly, like the controls, up to 32–64 cells. Up to this stage, blastomeres could be observed as unfused cells. Subsequently they looked like disorganized masses bearing sensorial granules (Fig. 7).

Gastrulae or neurulae, incubated for 1 h in 10⁻⁵ and 10⁻⁷ mol dm⁻³ Me₂SnClpenG solutions and then transferred to normal seawater, originated anomalous larvae with twisted and short tails (Fig. 8).

Bu₂SnClpenG

Eggs incubated for 15 min after fertilization in 10⁻⁵ and 10⁻⁷ mol dm⁻³ Bu₂SnClpenG solutions cleaved up to eight blastomeres which appeared to be different in size and occasionally tended to fuse. As a consequence, 24 h later eggs resembled an uncleaved lump. Moreover, the follicular cells which generally surround the eggs were absent as in the case of Me₂SnClpenG (Fig. 9).

Eggs incubated in 10⁻⁷ mol dm⁻³ solution cleaved but gave rise to anomalous embryos without tails, in the membranes and with small sensorial organs (Fig. 10).

Finally, gastrulae or neurulae incubated for 1 h in 10⁻⁵ mol dm⁻³ solution and then transferred into normal seawater developed as abnormal larvae with twisted and short tails.

Ph₂SnClpenG

Fertilized eggs incubated in 10⁻⁵ and 10⁻⁷ mol dm⁻³ Ph₂SnClpenG solutions originated anomalous embryos; some of those treated with 10⁻⁷ mol dm⁻³ solution had a short tail (Fig. 11). When gastrulae or neurulae were treated for 1 h and then transferred into normal seawater, they developed into anomalous larvae within the membranes, with short tails.

Me₃SnClpenGNa

Eggs incubated in 10⁻⁵ mol dm⁻³ Me₃SnClpenGNa solution stopped developing at the two–four cell stage. When eggs were treated with 10⁻⁷ mol dm⁻³ solution, 50% gave rise to anomalous embryos, some of which had pigment spots, and 40% blocked at an anomalous four-cell stage (Fig. 12). Gastrulae or neurulae incubated for 1 h in 10⁻⁵ mol dm⁻³ solutions originated anomalous embryos.

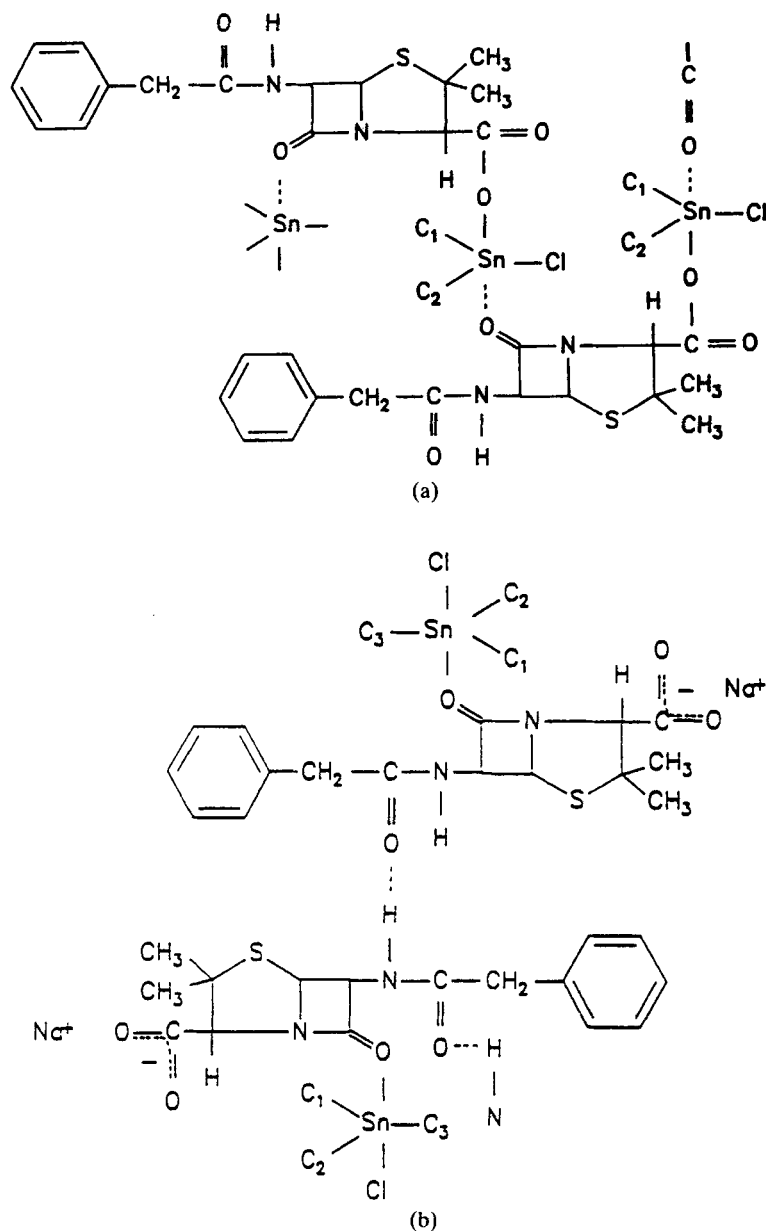


Figure 4 Proposed structures of $R_2\text{SnClpenG}$ (a) and $R_3\text{SnClpenGNa}$ (b) on the basis of the spectroscopic investigations.

$\text{Bu}_3\text{SnClpenGNa}$

Eggs incubated in $10^{-5} \text{ mol dm}^{-3}$ $\text{Bu}_3\text{SnClpenGNa}$ solution for 15 minutes after fertilization elongated but they remained uncleaved (Fig. 13), while eggs incubated in $10^{-7} \text{ mol dm}^{-3}$ solution blocked at the two-four-cell stage, at a different size. Gastrulae or neurulae incubated for 1 h in $10^{-5} \text{ mol dm}^{-3}$ solution,

gave rise to anomalous and disorganized embryos (Fig. 14)

$\text{Ph}_3\text{SnClpenGNa}$

Fertilized eggs treated with $10^{-5} \text{ mol dm}^{-3}$ $\text{Ph}_3\text{SnClpenGNa}$ solution did not elongate regularly before the cleaving process. Hence, they blocked at the two-three blastomere stage. Eggs



Figure 5 *Ciona intestinalis* control larvae (magnification $\times 50$).

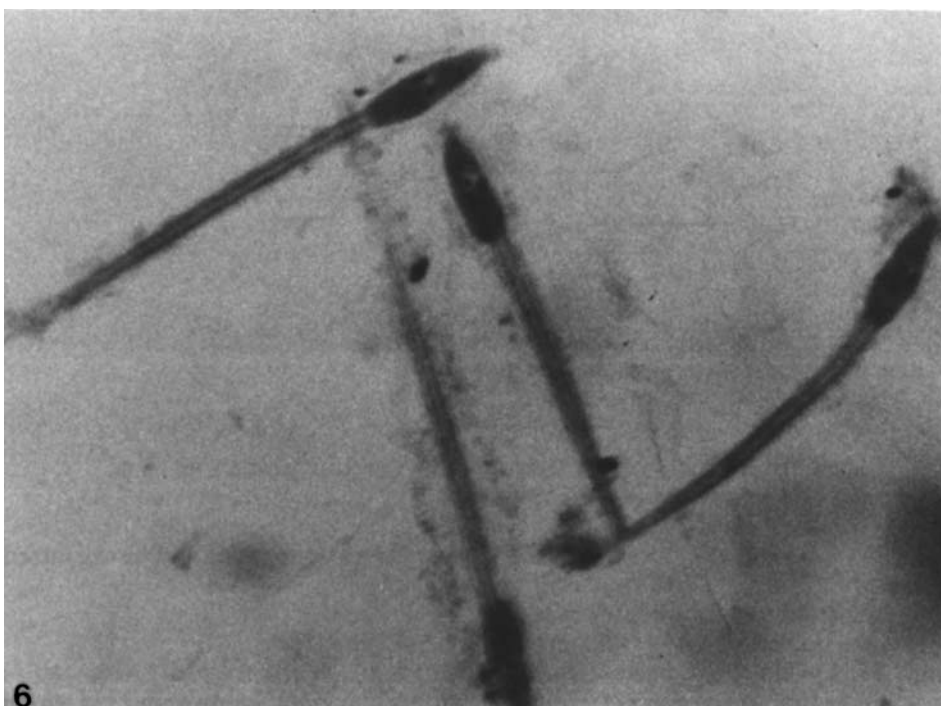


Figure 6 Larvae developed from eggs incubated for 15 min after fertilization in $10^{-5} \text{ mol dm}^{-3}$ penGNa solution (magnification $\times 50$).

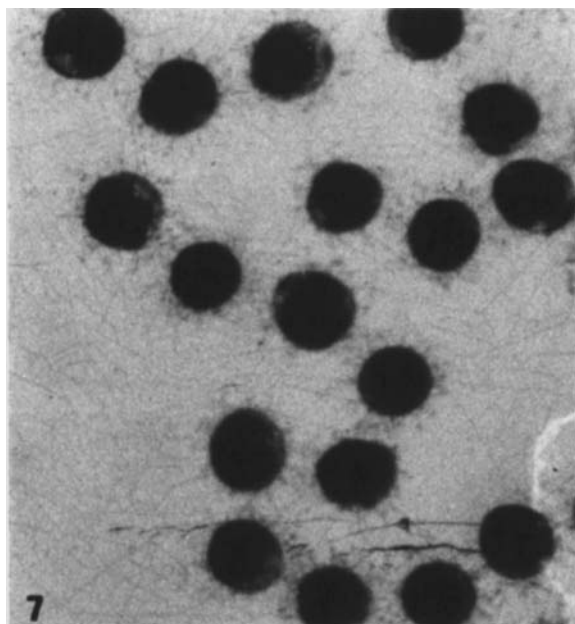


Figure 7 Anomalous embryos developed from eggs incubated after fertilization in $10^{-7} \text{ mol dm}^{-3} \text{ Me}_2\text{Sn(IV)ClpenG}$ solution (magnification $\times 50$).

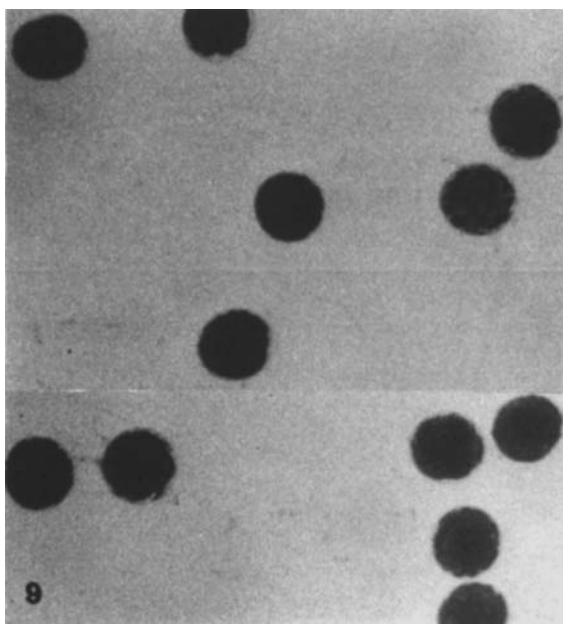


Figure 9 Eggs incubated in $10^{-5} \text{ mol dm}^{-3} \text{ Bu}_2\text{Sn(IV)ClpenG}$ solution after fertilization. They cleaved up to the 8-, 16- or 32-cell stage and afterwards stopped dividing. The follicular cells, which normally surround the eggs, are detached (magnification $\times 50$).

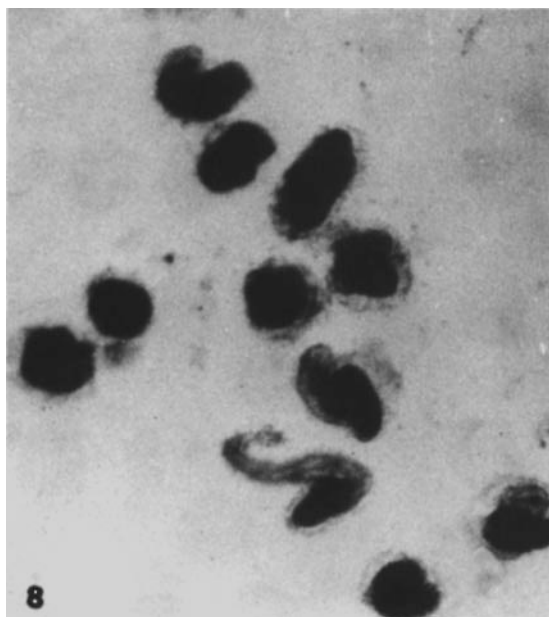


Figure 8 Gastrulae incubated for 1 h in $10^{-7} \text{ mol dm}^{-3} \text{ Me}_2\text{Sn(IV)ClpenG}$ solution and then transferred into normal seawater. Anomalous larva with twisted and short tails are clearly present (magnification $\times 50$).

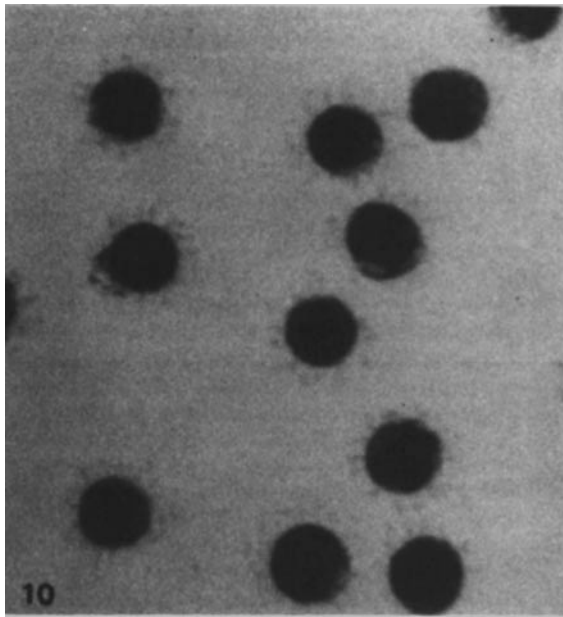


Figure 10 Anomalous embryos developed from eggs incubated after fertilization in $10^{-7} \text{ mol dm}^{-3} \text{ Bu}_2\text{Sn(IV)ClpenG}$ solution (magnification $\times 50$).

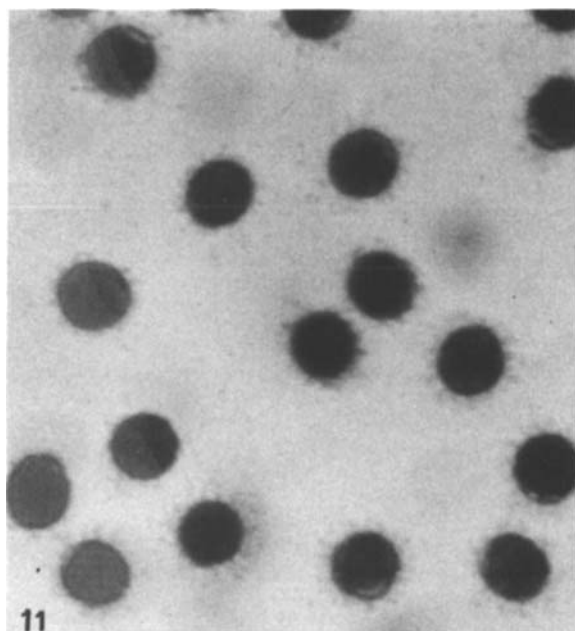


Figure 11 Anomalous embryos from eggs incubated after fertilization in $10^{-7} \text{ mol dm}^{-3} \text{ Ph}_2\text{Sn(IV)ClpenG}$ solution (magnification $\times 50$).

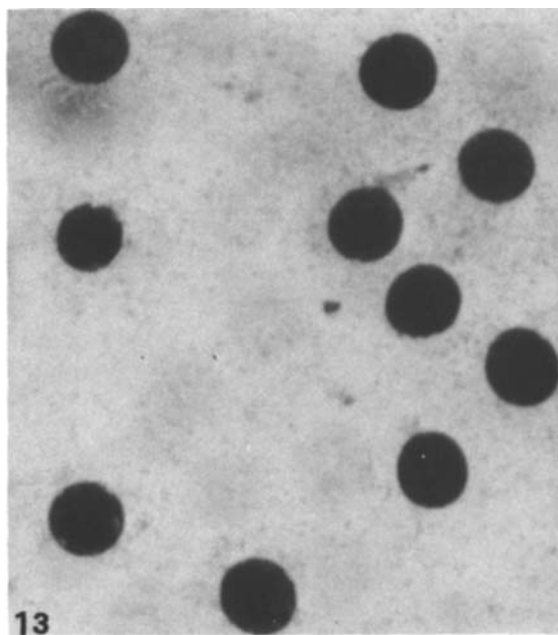


Figure 13 Uncleaved eggs incubated after fertilization in $10^{-5} \text{ mol dm}^{-3} \text{ Bu}_3\text{Sn(IV)ClpenGNa}$ solution (magnification $\times 50$).

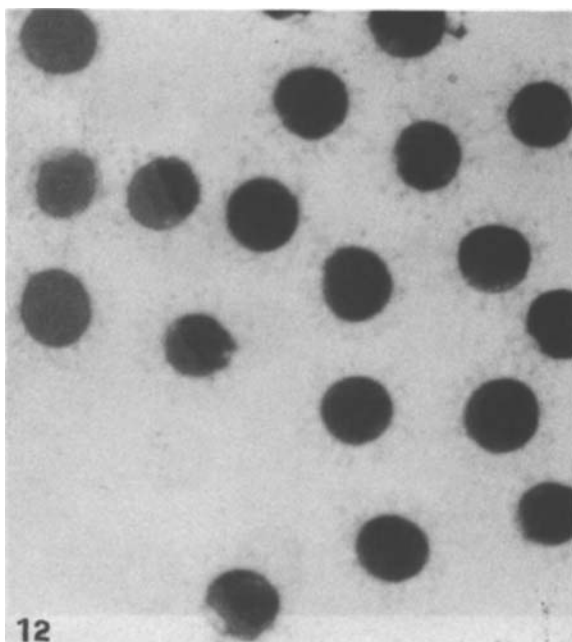


Figure 12 Anomalous embryos developed from eggs incubated in $10^{-7} \text{ mol dm}^{-3} \text{ Me}_3\text{Sn(IV)ClpenGNa}$ solution (magnification $\times 50$).

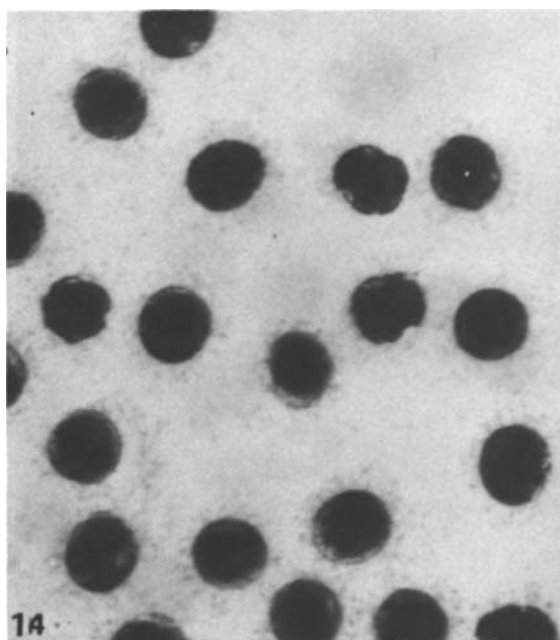


Figure 14 Anomalous embryos derived from gastrulae incubated for 1 h in $10^{-7} \text{ mol dm}^{-3} \text{ Bu}_3\text{Sn(IV)ClpenGNa}$ solution (magnification $\times 50$).

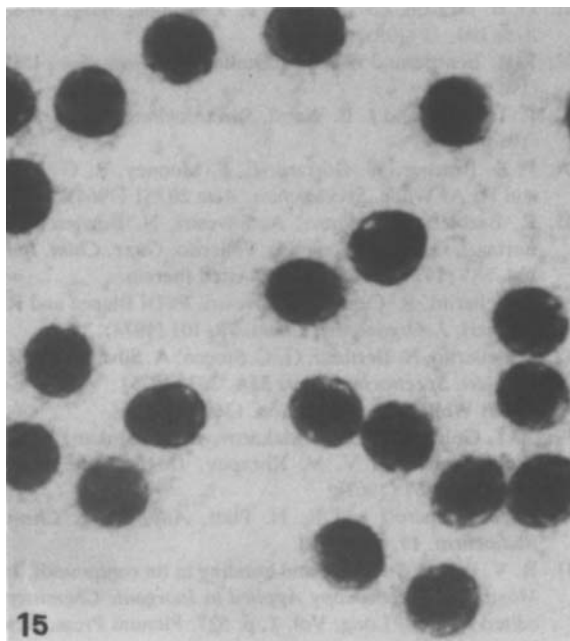


Figure 15 Anomalous embryos from fertilized eggs incubated in 10^{-7} mol dm $^{-3}$ Ph $_3$ Sn(IV)ClpenGNa solution (magnification $\times 50$).

incubated in 10^{-7} mol dm $^{-3}$ Ph $_3$ SnClpenGNa solution could be grouped as follows: 30% blocked at early developmental stages, while the remainder appeared as embryonic masses showing external sensorial granules (Fig. 15). Gastrulae or neurulae treated with 10^{-5} and 10^{-7} mol dm $^{-3}$ solutions gave rise to anomalous embryos. The anomalies were like those observed for Me $_3$ SnClpenGNa and Bu $_3$ SnClpenGNa.

Discussion

Results obtained from *in vivo* observations of *Ciona intestinalis* developing embryos suggested two main considerations. The first was that both diorganotin(IV)chloropenicillin G and triorganotin(IV)chloropenicillin G sodium derivatives are as toxic as the organotin(IV) parents, independently of the presence of the ligand. The second was that the toxicity responses to triorganotin(IV)chloropenicillin G sodium compounds were higher than those to diorganotin(IV)chloropenicillin G, and that in the diorganotin(IV) and triorganotin(IV) series, once again, the butyltin(IV) derivatives were the most active toxicants²³⁻²⁷ towards living animals, as already ascertained, *inter alia*, in ascidian developing embryos^{25,26} and in male gonads of *Truncatella*

subcylindrica (Mollusca, Mesogastropoda).⁶⁵ In the latter work, quantitative evaluations of chromosome abnormalities occurring during both mitotic and meiotic processes were given.

In the present report, genotoxicity of organotin(IV)chloropenicillin G compounds was unequivocally demonstrated by the fact that *Ciona intestinalis* fertilized eggs either blocked at early stages of development, or gave rise to anomalous larvae.

Since experiments carried out using both penicillin G sodium and penicillin G derivatives made it apparent that anomalies occurred exclusively after the use of the latter, we conclude that genotoxicity is presumably due to the organotin(IV)chloro moieties. More precisely, in agreement with previous studies developed on terrestrial and aquatic animals,⁶⁶ we believe that genotoxic effects can be related to the presence or organotin(IV) in these complexes.

Two major non-exclusive hypotheses can be advanced to explain the results of our work:

- (1) Consistent ultrastructural damage, involving the mitochondrial complexes and cytomembranes, might be induced by the heavy metal, tin, contained in the compounds.²⁶
- (2) Irregular cleaving processes might reflect damage affecting chromosome structure and polymerization of mitotic spindle tubulin during the first cell divisions. Chromosome aberrations, such as chromosome fragments, chromosome bridges and large decondensed chromosome regions, have been found in early developing embryos of *Anilocara physodes* (Crustacea, Isopoda), following exposure to bis[dimethyltin(IV)chloro]protoporphyrin IX.⁶⁷

Alternatively both events (1) and (2) might have occurred.

Acknowledgements Financial support by the Ministero per l'Università e la Ricerca Scientifica e Tecnologica, Roma, is gratefully acknowledged.

REFERENCES

1. J. C. Dabrowiak, F. T. Greenaway, F. S. Santillo and S. T. Crooke, *Biochem. Biophys. Res. Comm.* **91**, 721 (1979).
2. R. P. Pillai, N. R. Krishna, T. T. Sakai and J. D. Glickson, *Biochem. Biophys. Res. Comm.* **97**, 270 (1980).

3. D. Solaiman, E. A. Rao, W. Antholine and D. H. Petering, *J. Inorg. Biochem.* **12**, 201 (1980).
4. R. D. Bereman and M. E. Winkler, *J. Inorg. Biochem.* **13**, 95 (1980).
5. Y. Uehara, M. Hori and H. Umezawa, *Biochem. Biophys. Res. Comm.* **104**, 416 (1982).
6. F. Greenaway and J. C. Dabrowiak, *J. Inorg. Biochem.* **16**, 91 (1982).
7. L. Banci, A. Dei and D. Gatteschi, *Inorg. Chim. Acta* **67**, L53 (1982).
8. C. M. Vos, G. Westera and D. Schipper, *J. Inorg. Biochem.* **16**, 245 (1982).
9. B. Balko and G. W. Liesegang, *Biochem. Biophys. Res. Comm.* **110**, 827 (1983).
10. R. M. Burger, T. A. Kent, S. B. Horwitz, E. Munck and J. Peisack, *J. Biol. Chem.* **258**, 1559 (1983).
11. W. E. Antholine, J. S. Hyde, R. C. Sealy and D. H. Petering, *J. Biol. Chem.* **259**, 4437 (1984).
12. M. M. L. Fiallo and A. Garlette-Suillerot, *J. Inorg. Biochem.* **31**, 43 (1987).
13. S. Yamabe, Japanese Patent JP 01 93 590 [89 93 590] *Chem. Abstr.* 111 219 307z (1989).
14. H. Umezawa, in *Anticancer Agents Based on Based on Natural Product Models*, edited by J. M. Chassady and J. D. Duros, pp. 147–166. Academic Press, New York (1980).
15. G. S. Sodhi, R. K. Bajaj and N. K. Kaushik, *Inorg. Chim. Acta* **92**, L27 (1984).
16. S. G. Kamrah, S. Sodhi and N. K. Kaushik, *Inorg. Chim. Acta* **107**, 29 (1985) and references cited therein.
17. D. H. Brown and W. E. Smith, *Inorg. Chim. Acta* **93**, L29 (1984).
18. U. Deuschlel and U. Weser, *Inorg. Chim. Acta* **152**, 219 (1988).
19. R. Barbieri, A. Silvestri, F. Huber and C.-D. Hager, *Can. J. Spectrosc.* **26**, 194 (1981) and references cited therein.
20. G. Domazetis, R. J. Magee and B. D. James, *J. Organomet. Chem.* **162**, 239 (1978).
21. M. Asso, R. Panossian and M. Guillianio, *Spectrosc. Lett.* **17**, 271 (1984) and references cited therein.
22. L. Pellerito, S. Grimaudo, M. A. Girasolo, G. Dia and F. Huber, *Abstracts 3rd Swiss-Italian Meeting Inorg. Bioinorg. Chem.*, Ferrara, 6–7 June 1986, p. 34.
23. L. Pellerito, S. Grimaudo, M. A. Girasolo, G. Dia and C. Mansueto, *Abstracts, 28th Mössbauer Discussion Group Meeting, London, 13–15 July 1987*, p. 22.
24. L. Pellerito, *Abstracts 4th Swiss-Italian Meeting Inorg. Bioinorg. Chem.*, Neuchatel, 20–22 September 1988 PL9.
25. C. Mansueto, M. Lo Valvo, L. Pellerito and M. A. Girasolo, *Appl. Organomet. Chem.* **7**, 95 (1993).
26. C. Mansueto, M. Gianguzza, G. Dolcemascolo and L. Pellerito, *Appl. Organomet. Chem.*, **7**, 391 (1993).
27. W. P. Neuman, *Die Organische Chemie des Zinns*, Verlag, Stuttgart (1967).
28. W. Schöniger, *Microchim. Acta* **9**, 123 (1955).
29. D. D. Dexter and J. M. Van der Veen, *J. Chem. Soc. Perkin I* 185 (1978) and references cited therein.
30. G. B. Deacon and R. J. Phillips, *Coord. Chem. Rev.* **33**, 227 (1980).
31. G. B. Deacon, F. Huber and R. J. Phillips, *Inorg. Chim. Acta* **104**, 41 (1985).
32. I. R. Beattie and G. P. McQuillan, *J. Chem. Soc.* 1519 (1963).
33. P. Taimsalu and J. L. Wood, *Spectrochim. Acta* **20**, 1045 (1964).
34. F. K. Butcher, W. Gerrard, E. F. Mooney, R. G. Rees and H. A. Willis, *Spectrochim. Acta* **20**, 51 (1964).
35. R. Barbieri, G. Alonzo, A. Silvestri, N. Burriesci, N. Bertazzi, G. C. Stocco and L. Pellerito, *Gazz. Chim. Ital.* **104**, 885 (1974) and references cited therein.
36. L. Pellerito, R. Cefalù, A. Silvestri, F. Di Bianca and R. Barbieri, *J. Organomet. Chem.* **78**, 101 (1974).
37. L. Pellerito, N. Bertazzi, G. C. Stocco, A. Silvestri and R. Barbieri, *Spectrochim. Acta* **31A**, 303 (1975).
38. D. H. Whiffen, *J. Chem. Soc.* 1350 (1956).
39. V. I. Goldanskii, E. F. Makarov, R. A. Stukan, V. A. Trukhatanov and V. V. Khrapov, *Dokl. Akad. Nauk SSSR* **151**, 357 (1963).
40. G. M. Bancroft and R. H. Platt, *Adv. Inorg. Chem. Radiochem.* **15**, 59 (1972).
41. R. V. Parish, Structure and bonding in tin compounds. In *Mössbauer Spectroscopy Applied to Inorganic Chemistry*, edited by G. J. Long, Vol. 1, p. 527. Plenum Press, New York (1984).
42. G. M. Bancroft, V. G. Das Kumar, T. K. Sham and M. G. Clark, *J. Chem. Soc., Dalton Trans.* 643 (1976) and references cited therein.
43. M. G. Clark, A. G. Maddock and R. H. Platt, *J. Chem. Soc., Dalton Trans.* 281 (1972).
44. H. A. Bent, *J. Inorg. Nucl. Chem.* **19**, 43 (1961).
45. E. L. Muetterties and R. A. Schunn, *Quart. Rev.* **20**, 245 (1966).
46. R. L. Collins and J. C. Travis, The electric field gradient tensor. In *Mössbauer Effect Methodology*, edited by I. J. Gruverman, Vol. 3, p. 123. Plenum Press, New York (1967).
47. R. Barbieri, L. Pellerito and F. Huber, *Inorg. Chim. Acta* **30**, L321 (1978).
48. W. L. Jolly and W. B. Perry, *J. Am. Chem. Soc.* **95**, 5442 (1973).
49. W. L. Jolly and W. B. Perry, *Inorg. Chem.* **13**, 2686 (1974).
50. W. B. Perry and W. L. Jolly, The calculation of atomic charge in molecules by an electronegativity equalization procedure: a description of program CHELEQ. US Atomic Energy Comm., Contract W-7405-ENG-48 (Nov. 1974).
51. R. Barbieri and A. Silvestri, *Inorg. Chim. Acta* **47**, 201 (1981).
52. J. L. Lefferts, K. C. Molloy, M. B. Hossain, D. Van der Helm and J. J. Zuckerman, *J. Organomet. Chem.* **240**, 349 (1982).
53. N. Kasai, K. Yasuda and R. Okawara, *J. Organomet. Chem.* **179**, 145 (1979).
54. E. O. Schlemper and D. Britton, *Inorg. Chem.* **5**, 507 (1966).
55. Y. M. Chow and D. Britton, *Acta Crystallogr., Sect. B* **27**, 856 (1971).

56. R. A. Forder and G. M. Sheldrick *J. Organomet. Chem.* **21**, 115 (1970).
57. A. M. Domingos and G. M. Sheldrick, *J. Organomet. Chem.* **65**, 257 (1974).
58. T. N. Tarkhova, E. V. Chupronov, M. A. Simonov and N. V. Belov, *Soviet Phys. Crystallogr.* **22**, 2306 (1977).
59. R. Barbieri, A. Silvestri, G. Ruisi and G. Alonzo, *Inorg. Chim. Acta* **97**, 113 (1986) and references cited therein.
60. R. Barbieri and A. Silvestri, *J. Chem. Soc., Dalton Trans.* 1019 (1984).
61. J. N. R. Ruddick and J. R. Sams, *J. Chem. Soc., Dalton Trans.* 470 (1970).
62. V. G. Kumar Das, N. V. Weng, P. J. Smith and R. Hill, *J. Chem. Soc. Dalton Trans.* 552 (1981).
63. R. C. Poller and J. N. R. Ruddick, *J. Chem. Soc. A* 2273 (1969).
64. F. P. Mullins and C. Curran, *Inorg. Chem.* **7**, 2584 (1968).
65. R. Vitturi, C. Mansueto, E. Catalano, L. Pellerito and M. A. Girasolo, *Appl. Organomet. Chem.* **6**, 525 (1992).
66. C. J. Sindermann, *Principal Diseases of Marine Fish and Shellfish*, 2nd edn, Vol. 1, pp. 409–410. Academic Press, San Diego, CA (1990) and references cited therein.
67. R. Vitturi, E. Catalano, M. R. Lo Conte and L. Pellerito, *Appl. Organomet. Chem.* **7**, 295 (1993).